NJC

Accepted Manuscript

This is an *Accepted Manuscript*, which has been through the Royal Society of Chemistry peer review process and has been accepted for publication.

Accepted Manuscripts are published online shortly after acceptance, before technical editing, formatting and proof reading. Using this free service, authors can make their results available to the community, in citable form, before we publish the edited article. We will replace this *Accepted Manuscript* with the edited and formatted *Advance Article* as soon as it is available.

You can find more information about *Accepted Manuscripts* in the Information for Authors.

Please note that technical editing may introduce minor changes to the text and/or graphics, which may alter content. The journal's standard Terms & Conditions and the Ethical guidelines still apply. In no event shall the Royal Society of Chemistry be held responsible for any errors or omissions in this *Accepted Manuscript* or any consequences arising from the use of any information it contains.

ROYAL SOCIETY OF CHEMISTRY

www.rsc.org/njc

Synthesis and Optical Properties of Nitrogen and Sulfur Co-doped Graphene Quantum Dots

Schematic and digital photos of the preparation for NS-GQDs. Sulfur plays a meritorious role in enhancing the photoluminescence of NS-GQDs.

NJC RSC

ARTICLE

Synthesis and Optical Properties of Nitrogen and Sulfur Co-doped Graphene Quantum Dots

Ben-Xing Zhang,[a] Hui Gao*[a] and Xiao-Long Li[b]

Strong blue luminescence and water-soluble nitrogen (N) and sulfur (S) co-doped graphene quantum dots (NS-GQDs) were fabricated via a one-step hydrothermal method using oxidized graphene. Ammonia and S powder were selected as the source of N and S, respectively. The results indicated that both N and S atoms were successfully incorporated into the sp^2-hybridized carbon framework of graphene. Under the excitation of 365 nm, the maximum emission intensity could be obtained with the atomic ratio of N/S being 1:1.2. The as-prepared NS-GQDs exhibit brighter luminescence compared with N-doped graphene quantum dots (N-GQDs). S-doping play an important role for enhancing the emission intensity of NS-GQDs. In addition, the luminescence property shows exceptional resistance to high salt concentration. These virtues bring NS-GQDs to be exploited in bio-imaging, solar cells and ion detection.

1 Introduction

Graphene quantum dots (GQDs), as the latest member of the carbon (C) family, are drawing tremendous research interest resulting from the numbers of unique properties, including abundant availability, satisfying water solubility, robust chemical inertness, low cytotoxicity, excellent biocompatibility and resistance to photobleaching. These GQDs have been exploited in a wide range of applications: ion detection,[1, 2] photovoltaic devices,[3] bio-sensing,[4, 5] bio-imaging[6] and deoxyribonucleic acid (DNA) cleavage,[7] to name a few. But when contrasted with semiconductor quantum dots, the GQDs' luminescence property is not satisfying.[8] Loh and co-workers[9] demonstrated that the isolated clusters with numbered atoms were closely related to the absorption of photons and the structural defects are crucial to the creation of these clusters. Therefore the relatively low defects (active sites) of undoped GQDs are to blame for deficient optical properties. Doping heteratoms including boron,[10] nitrogen (N),[10, 11] fluorine[12] and sulfur (S)[13] is among the most practical strategy to introduce more defects, modify the electron density and tailor photic property of GQDs. It will be highly interesting to explore what will happen when the doped element (N, S) has the similar radius (radius of C: 0.77 Å, N: 0.75 Å) or electronegativity (electronegativity of C: 2.55, S: 2.58) with C.

To date, various synthesis strategies of GQDs and doping GQDs mainly including the top-down and the bottom-up methods have been proposed. The former refers to cutting high dimensional carbon materials into zero dimensional GQDs via hydrothermal methods,[14] electrochemical strategies,[15] oxygen (O) plasma treatment[16] and stripping of oxidized debris[17]. On the other hand, microwave-assisted hydrothermal method,[18] thermal pyrolysis[19] and cage opening of fullerenes[20] are classified into the bottom-up routes, namely carbonizing some designated organic precursors. So far, research attention was mainly paid on N-doped graphene quantum dots (N-GQDs) while NS-GQDs have been hardly investigated. Of late, Qu *et al*.[13] demonstrated that N and S co-doped graphene quantum dots (NS-GQDs) have been synthesized triumphantly by the bottom-up approaches with its NS-GQDs exhibiting high quantum yield (71%) and outstanding visible light photocatalysts. Nevertheless, compared with the top-down approaches, the bottom-up methods usually suffer from severe synthetic conditions and requirement for special precursors. To our knowledge, the field of top-down method for preparing NS-GQDs has been rarely researched. Herein, we present a feasible process to synthesis NS-GQDs in an autoclave using oxidized graphene (GO), ammonia (as N source and passivation agent[21]) and S powder (as S source). The results show that S has been introduced into the framework successfully. NS-GQDs with different photoluminescence (PL) intensity were prepared by varying the mass ratios of GO, S powder and ammonia solution. The as-prepared N-GQDs and NS-GQDs show excited wavelength dependent PL behavior. It is implying that N-GQDs and NS-GQDs may have the same PL origin according to the function relationship between the excitation and emission wavelength of both GQDs.

2 Experimental

Graphite and S powder were purchased from Sinopharm Chemical Reagent Co., Ltd. All chemicals were of analytical reagent without further note and used as received. Deionized water used in the whole experiment holds the resistivity no lower than 18.1 MΩ*cm. GO were prepared by improved Hummers' method.[22, 23]

2.1 Preparation of samples (a series of NS-GQDs with different PL intensity)

In a typical preparation procedure, the mixture of GO solution (20 ml, 3.0 mg/ml), ammonia solution (0.6 ml, 28 wt%) and S (the weight of S powder: 0.100 g for N-S-1 sample, 0.070 g for N-S-2 sample, 0.050 g for N-S-3 sample, 0.030 g for N-S-4 sample, 0.010 g for N-S-5 sample, 0.005 g for N-S-6 sample, 0.003 g for N-S-7 sample and 0.001 g for N-S-8 sample, respectively) was stirred to

form a homogeneous solution and transferred into a Teflon-lined autoclave. The sealed autoclave was maintained at 180 ˚C for 12 h in an electric oven. Columnar black sediment (reduced GO) was removed by millipore membrane (0.02 μm). The obtained supernatant was collected and dialyzed against deionized water to eliminate excess ammonia, sulfate radical and carbonate ion. We also prepared N-GQDs without the addition of S for the comparison.

2.2 Apparatus

Deionized water was gained from Millipore Elix 5 UV and Milli-Q Gradient Ultra-pure Water System. The Fourier transform infrared (FT-IR) spectra were registered between 500 and 4000 cm^{-1} on a FT-IR spectrometer (Nicolet NEXUS 670) using KBr pellets. The transmission electron microscopy (TEM) observation was made on a F-30 S-TWIN electron microscope (Tecnai G2, FEI Company). X-ray photoelectron spectra (XPS, PHI-5702, Physical Electronics) were obtained using a monochromated Al-Kα irradiation. UV-Vis absorption spectra were performed on a Perkin Elmer 950 spectrophotometer. Raman scattering spectra were obtained using a Renishaw InVia Raman microscope with 532 nm line of an Ar ion laser as an excitation source. The PL spectra and fluorescence emission spectra were recorded on an FLS-920T fluorescence spectrophotometer and a HORIBA JOBIN YVON Fluorolog-3 Spectrofluorometer system respectively. The decay curve was recorded on a PR305 phosphorophotometer. All the measurements were performed at room temperature.

3 Results and discussion

In this paper, we prepared N-GQDs and a series of NS-GQDs with different S content to investigate the S-doping-effect on optical property for GQDs. Schematic for the preparation of NS-GQDs is illustrated in Fig. 1. GO solution was prepared by a modified Hummer's method. Then, oxidized debris (the pink part) can be detached from GO under alkaline condition. NS-GQDs were finally obtained after the mixture of oxidized debris, S powder and ammonia solution were further treated through a hydrothermal process.

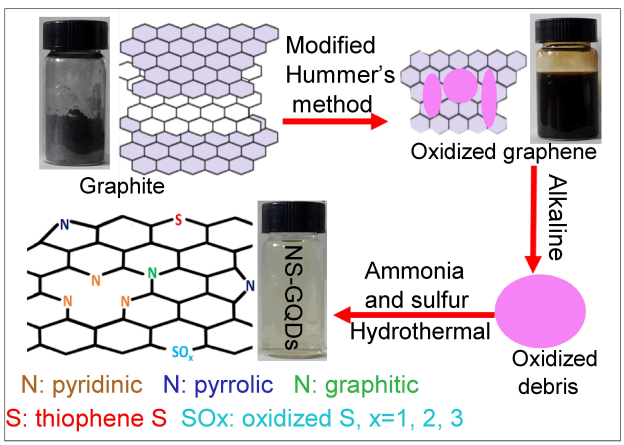

Fig. 1 Schematic and digital photos of the preparation for NS-GQDs. The location and chemical state of N and S in NS-GQDs.

A series of NS-GQDs with different PL intensity (same concentration) is shown in the inset of Fig. 2c (excited with 365 nm). As we can see, relationship between the content of S and PL intensity is not always a positive correlation (Fig. 2d). With the increase of S, there is an optimal mass ratio of raw materials with the corresponding mass of sulfur powder being 0.030 g. Although the fluorescence mechanism of GQDs is not completely understood, we can put forward a possible hypothesis: As the increase of S content, the defects quantity escalates, which contributed to the stronger emission intensity. However, at the same time, distance between adjacent defects diminish. When the content of S reaches up to *ca.* 30.4 wt%, the distance being short enough for electrons and holes to cross and recombine (energized by photons), the availability of excitation light source decline.

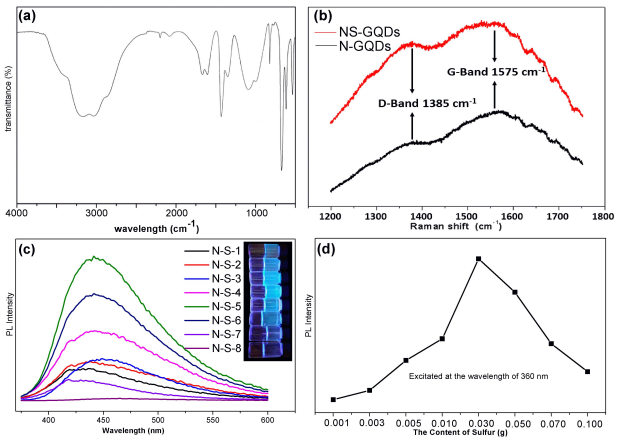

Fig. 2 The FT-IR spectrum of NS-GQDs (a) and Raman spectra (b) of N-GQDs and NS-GQDs. The PL spectra (c) of a series of NS-GQDs excited at 365 nm. (d) PL peak intensity versus the content of S for NS-GQDs.

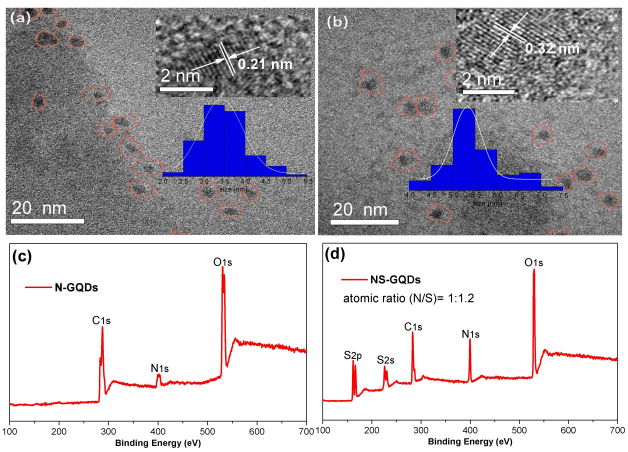

Fig. 3 TEM images of N-GQDs (a) and NS-GQDs (b). Insets are the corresponding high-resolution TEM images and size distributions, respectively. XPS full-spectra of N-GQDs (c) and NS-GQDs (d).

Unless otherwise stated, N-GQDs and NS-GQDs (labeled as: N-S-4) with strongest luminescence were selected for various characterizations. TEM images of both N-GQDs and NS-GQDs are shown in Fig. 3a, b. High-resolution TEM photographs (insets of Fig. 3a, b) reveal discernible lattice structures with the lattice space of 0.32 nm, which is corresponded with graphite (002) plane, while 0.21 nm consistent with in-plane lattice spacing of graphene. These consequences are coincided with many other reported GQDs prepared by the bottom-up methods.[24-26] Therefore, N-GQDs and NS-GQDs may possess the similar structure. Size distribution analysis (Gaussian fitting) point out that N-GQDs and NS-GQDs are quasi-spherical with a mean radius of 3.16 nm (range from 2.42 nm

to 5.35 nm) and 5.25 nm (range from 4.40 nm to 7.26 nm), respectively.

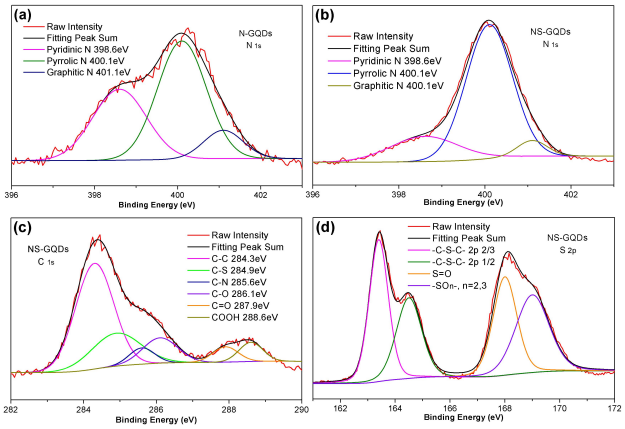

Fig. 4 (a) and (b) are the high-resolution N 1s spectra of N-GQDs and NS-GQDs, respectively. Detailed C 1s (c) and S 2p (d) spectra of NS-GQDs.

As we can obtain in XPS full-spectra (Fig. 3c, d), peaks at 533 eV (O 1s), 400 eV (N 1s), and 284 eV (C 1s) are present in both N-GQDs and NS-GQDs, additional peaks at *ca*. 164 eV (S 2p) and 227 eV (S 2s) observed in the NS-GQDs.[13, 27, 28] This indicated that S has been doped into the framework successfully. In Fig. 4a, b, the high-resolution spectra of N 1s (both N-GQDs and NS-GQDs) can be divided into three peaks at: 398.6 eV, 400.1 eV and 401.1 eV, assigned to pyridinic N, pyrrolic N and graphitic N, respectively.[29-31] S 2p spectrum (Fig. 4d) present -C-S-C-2p 2/3 (163.4 eV), -C-S-C-2p 1/2 (164.5 eV), S=O (168.0 eV), and -SO_n-, n=2,3 (169.0 eV) peaks, in line with previous reports,[32-34] therefore, S is present in two distinct forms: thiophene S (-C-S-C-) and oxidized S (-C-SO_x-C-, x=1, 2, 3). No peaks relative to S can be detected in the fine S 2p spectra of N-GQDs (Fig. S1a). It is a noteworthy fact that the content of O and N increases with the introduction of S. The following two reasons account for this phenomenon. One is the creation of oxide groups (oxidized S such as sulfate or sulfonate). Another is that S-doping may bring more active graphene sites which are easier to bond with N or O. As shown in fine C 1s spectra (Fig. 4c and Fig. S1b), C exists in at least 5 diverse chemical states,[11, 35, 36] including the formation of carbonyls and carboxylates. These polar groups account for GQDs' admirable water-solubility. In FT-IR spectra (Fig. 2a), peaks around 3300 cm^{-1} (stretching vibrations of N-H and O-H) also explain the exceptional hydrophilic properties. The state of S is further confirmed basing on the featured peaks 1096 cm^{-1} (stretching vibrations of S=O) and 635 cm^{-1} (stretching vibrations of C-S).[13] Absorption in the realm of 1580 cm^{-1} to 1720 cm^{-1} are attributed to vibrations of C=C, C=N and C=O,[28] in agreement with above XPS data. Beyond that, stretching vibrations of C-N are observed at 1400 cm^{-1}. Long-term stability (Fig. S2) was put down to strong interaction among atoms and polar groups. Raman spectra are posted in Fig. 2b (fluorescence background was corrected through an intelligent algorithm[37]). The relative intensity of the disorder (D) band and the graphite (G) band (I_D/I_G) of N-GQDs and NS-GQDs is 0.74 and 0.89, respectively, which indicated that NS-GQDs have more defects than N-GQDs.

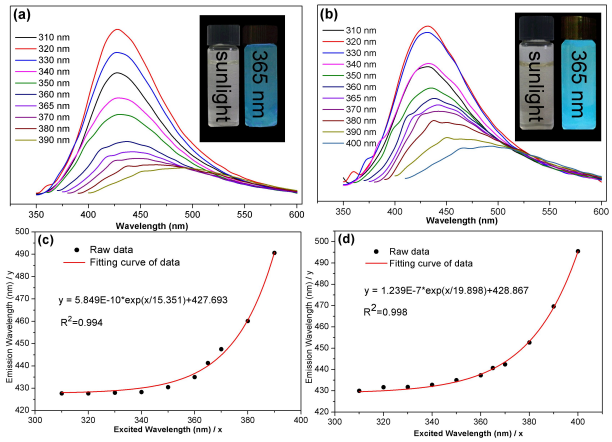

Fig. 5 The PL spectra of N-GQDs (a) and NS-GQDs (b) and detailed relationship between the excitation and emission wavelength of N-GQDs (c) and NS-GQDs (d). Insets of (a) and (b) are digital photos of N-GQDs and NS-GQDs.

PL excitation (PLE) spectra of NS-GQDs show a wide peak around 320 nm (Fig. S3). Excited wavelength dependent PL behavior is observed in both N-GQDs and NS-GQDs (Fig. 5). In the case of NS-GQDs, the emission wavelength shifts from 430 nm to 496 nm when the excitation wavelength increases gradually from 310 nm to 400 nm with the maximum excitation wavelength of 320 nm and the corresponding emission wavelength at 432 nm. The results are coincident with the PLE data. It has been reported that the size and the surface state are the explanation for this novel property earlier.[25] But lately, Tang and his colleagues[38] indicated that the inter-system crossing and adjacent vibrational relaxation of excited electron are to blame for this behavior. Further details about the relationship between the excitation and emission wavelength are demonstrated in Fig. 5c,d. Both data strictly conform to the non-linear fitting formula of y = A*exp(x/B)+C. Taking advantage of this precise function, we can approximately reckon the excitation wavelength for the sake of gaining a specific wavelength of emission or appointed color when these GQDs are applied to bio-imaging. What's more, the lifetime (excited with 330 nm) complying with tri-exponential decay of N-GQDs (5.9 ns) and NS-GQDs (5.4 ns) is close (Fig. S4a, b). Thus it is reasonable to believe that N-GQDs and NS-GQDs may have the same the PL origin: isolated molecular cluster that has been proved to benefit transport by hopping.[9]

Fig. S5 shows absorption curves of NS-GQDs. The peaks at 235 nm ($\pi \rightarrow \pi^*$ of conjugated diene), 280 nm ($\pi \rightarrow \pi^*$ of C=N) and 324 nm ($n \rightarrow \pi^*$ of C=O) are observed. The addition of N brings new energy level which is essential to the absorption at 274 nm. The N energy level acts as "bridge" in altering the electrocatalytic activity. Different with previous report[13], S-relative peaks around 550 nm and 595 nm are absent. The electronegativity of S and C atoms are so close that the discrepancy of both energy levels is negligible,[39] which result in the absence of S-relative peaks (Fig. S6). In addition, PL quantum yield of N-GQDs and NS-GQDs is *ca.* 10.1% and *ca.* 18.6%, respectively.

Nevertheless, the fluorescence intensity of NS-GQDs is markedly enhanced compared with N-GQDs excited with 365 nm (insets of Fig5. a,b). Obviously, S-dopant may give reason to the difference. The defects of GQDs increase with the introduction of S according to the Raman spectra. These defects are positive charged sites that are essential to optical property.[40]

As shown in Fig. S7, The NS-GQDs exhibit bright PL emission in the water solution of neutral and alkaline conditions. There is slightly muddy in acidic pH solution and the intensity of the emission peaks decrease sharply. Interestingly, emission wavelength shifts from 420 nm to 445 nm when the pH value decreases from 8 to 6. It has been reported that pH-dependent behavior may be attributed to the aggregation of GQDs because of the adherent oxygen-containing groups.[41] In addition, NS-GQDs exhibit excellent PL stability at high salt concentration (Fig. S8). These virtues enrich the application in pH sensor and other utilizations under extreme environmental conditions.

4 Conclusions

In brief, we have developed a feasible one-step method to prepare nitrogen and sulfur co-doped graphene quantum dots (NS-GQDs) via oxidized debris stripping from oxidized graphene in the presence of sulfur powder and ammonia solution. The as-prepared nitrogen and sulfur co-doped graphene quantum dots displays amazing enhancement luminescence at the side of nitrogen doped graphene quantum dots (N-GQDs). Sulfur is regarded as the most meritorious role. Both N-GQDs and NS-GQDs showed excitation-independent emission and tri-exponential function lifetime giving the credit to the similar PL origin. In addition, the different sulfur loads do not give a straight correlation with emission intensity. NS-GQDs with best performance in fluorescence hold the optimum atomic ratio of N/S (1:1.2). The synthesized NS-GQDs display well accepted PL nature, brilliant biocompatibility and excellent PL stability at high salt concentration, rendering a potential application in biomedicine, bio-imaging, bio-sensing, *etc*.

5 Acknowledgements

This work was financially supported by the Fundamental Research Funds for Central Universities (lzujbky-2013-186), the Natural Science Foundation of Gansu Province, China (Grant No. 1208RJYA005), the National Basic Research Program of China (973 program) (2010CB934501) and the Natural Science Foundation of China (11205235).

6 Notes and references

[a] School of Physical Science and Technology, Key Labortory for Magnetism and Magnetic Materials of Ministry of Education, Lanzhou University, Lanzhou 730000, P. R. China
E-mail: hope@lzu.edu.cn; Fax: +81 931 8913554; Tel: +81 931 8912772
[b] Shanghai Synchrotron Radiation Facility, Shanghai Institute of Applied Physics, Chinese Academy of Sciences, Shanghai 201204, P. R. China
† Electronic Supplementary Information (ESI) available. See DOI: 10.1039/b000000x/

1. Y.-L. Zhang, L. Wang, H.-C. Zhang, Y. Liu, H.-Y. Wang, Z.-H. Kang and S.-T. Lee, *RSC Advances*, 2013, 3, 3733.
2. R. Liu, H. Li, W. Kong, J. Liu, Y. Liu, C. Tong, X. Zhang and Z. Kang, *Materials Research Bulletin*, 2013, 48, 2529-2534.
3. Y. Li, Y. Hu, Y. Zhao, G. Shi, L. Deng, Y. Hou and L. Qu, *Advanced materials*, 2011, 23, 776-780.
4. H. Zhao, Y. Chang, M. Liu, S. Gao, H. Yu and X. Quan, *Chemical communications*, 2013, 49, 234-236.
5. J. Shen, Y. Zhu, X. Yang and C. Li, *Chemical communications*, 2012, 48, 3686-3699.
6. S. Zhu, J. Zhang, C. Qiao, S. Tang, Y. Li, W. Yuan, B. Li, L. Tian, F. Liu, R. Hu, H. Gao, H. Wei, H. Zhang, H. Sun and B. Yang, *Chemical communications*, 2011, 47, 6858-6860.
7. X. J. Zhou, Y. Zhang, C. Wang, X. C. Wu, Y. Q. Yang, B. Zheng, H. X. Wu, S. W. Guo and J. Y. Zhang, *Acs Nano*, 2012, 6, 6592-6599.
8. W.-d. Sheng, M. Korkusinski, A. D. Güçlü, M. Zielinski, P. Potasz, E. S. Kadantsev, O. Voznyy and P. Hawrylak, *Frontiers of Physics*, 2011, 7, 328-352.
9. K. P. Loh, Q. Bao, G. Eda and M. Chhowalla, *Nature chemistry*, 2010, 2, 1015-1024.
10. S. Dey, A. Govindaraj, K. Biswas and C. N. R. Rao, *Chemical Physics Letters*, 2014, 595-596, 203-208.
11. Y. Li, Y. Zhao, H. Cheng, Y. Hu, G. Shi, L. Dai and L. Qu, *Journal of the American Chemical Society*, 2012, 134, 15-18.
12. Q. Feng, Q. Cao, M. Li, F. Liu, N. Tang and Y. Du, *Applied Physics Letters*, 2013, 102, 013111.
13. D. Qu, M. Zheng, P. Du, Y. Zhou, L. Zhang, D. Li, H. Tan, Z. Zhao, Z. Xie and Z. Sun, *Nanoscale*, 2013, 5, 12272-12277.
14. D. Pan, J. Zhang, Z. Li and M. Wu, *Advanced materials*, 2010, 22, 734-738.
15. M. Zhang, L. Bai, W. Shang, W. Xie, H. Ma, Y. Fu, D. Fang, H. Sun, L. Fan, M. Han, C. Liu and S. Yang, *Journal of Materials Chemistry*, 2012, 22, 7461.
16. T. Gokus, R. R. Nair, A. Bonetti, M. Bohmler, A. Lombardo, K. S. Novoselov, A. K. Geim, A. C. Ferrari and A. Hartschuh, *Acs Nano*, 2009, 3, 3963-3968.
17. C. Hu, Y. Liu, Y. Yang, J. Cui, Z. Huang, Y. Wang, L. Yang, H. Wang, Y. Xiao and J. Rong, *Journal of Materials Chemistry B*, 2013, 1, 39.
18. L. B. Tang, R. B. Ji, X. K. Cao, J. Y. Lin, H. X. Jiang, X. M. Li, K. S. Teng, C. M. Luk, S. J. Zeng, J. H. Hao and S. P. Lau, *Acs Nano*, 2012, 6, 5102-5110.
19. R. L. Liu, D. Q. Wu, X. L. Feng and K. Mullen, *Journal of the American Chemical Society*, 2011, 133, 15221-15223.
20. J. Lu, P. S. Yeo, C. K. Gan, P. Wu and K. P. Loh, *Nature nanotechnology*, 2011, 6, 247-252.
21. G. S. Kumar, R. Roy, D. Sen, U. K. Ghorai, R. Thapa, N. Mazumder, S. Saha and K. K. Chattopadhyay, *Nanoscale*, 2014, 6, 3384-3391.
22. W. S. Hummers and R. E. Offeman, *Journal of the American Chemical Society*, 1958, 80, 1339-1339.
23. N. I. Kovtyukhova, P. J. Ollivier, B. R. Martin, T. E. Mallouk, S. A. Chizhik, E. V. Buzaneva and A. D. Gorchinskiy, *Chemistry of Materials*, 1999, 11, 771-778.
24. Y. Q. Dong, H. C. Pang, H. B. Yang, C. X. Guo, J. W. Shao, Y. W. Chi, C. M. Li and T. Yu, *Angew Chem Int Edit*, 2013, 52, 7800-7804.
25. P. Russo, A. M. Hu, G. Compagnini, W. W. Duley

and N. Y. Zhou, *Nanoscale*, 2014, 6, 2381-2389.
26. H. Ding, L. W. Cheng, Y. Y. Ma, J. L. Kong and H. M. Xiong, *New J Chem*, 2013, 37, 2515-2520.
27. Y. Dong, H. Pang, H. B. Yang, C. Guo, J. Shao, Y. Chi, C. M. Li and T. Yu, *Angewandte Chemie*, 2013, 52, 7800-7804.
28. D. Sun, R. Ban, P. H. Zhang, G. H. Wu, J. R. Zhang and J. J. Zhu, *Carbon*, 2013, 64, 424-434.
29. H. Gao, L. Song, W. Guo, L. Huang, D. Yang, F. Wang, Y. Zuo, X. Fan, Z. Liu, W. Gao, R. Vajtai, K. Hackenberg and P. M. Ajayan, *Carbon*, 2012, 50, 4476-4482.
30. Y. Chen, J. Wang, H. Liu, M. N. Banis, R. Li, X. Sun, T.-K. Sham, S. Ye and S. Knights, *The Journal of Physical Chemistry C*, 2011, 115, 3769-3776.
31. R. J. J. Jansen and H. Vanbekkum, *Carbon*, 1995, 33, 1021-1027.
32. Y. Su, Y. Zhang, X. Zhuang, S. Li, D. Wu, F. Zhang and X. Feng, *Carbon*, 2013, 62, 296-301.
33. J. Liang, Y. Jiao, M. Jaroniec and S. Z. Qiao, *Angewandte Chemie*, 2012, 51, 11496-11500.
34. Z. Yang, Z. Yao, G. Li, G. Fang, H. Nie, Z. Liu, X. Zhou, X. a. Chen and S. Huang, *Acs Nano*, 2011, 6, 205-211.
35. S. Dey, P. Chithaiah, S. Belawadi, K. Biswas and C. N. R. Rao, *Journal of Materials Research*, 2013, 29, 383-391.
36. Q. Liu, B. Guo, Z. Rao, B. Zhang and J. R. Gong, *Nano letters*, 2013, 13, 2436-2441.
37. Z.-M. Zhang, S. Chen, Y.-Z. Liang, Z.-X. Liu, Q.-M. Zhang, L.-X. Ding, F. Ye and H. Zhou, *Journal of Raman Spectroscopy*, 2009, 41, 659-669.
38. L. B. Tang, R. B. Ji, X. M. Li, K. S. Teng and S. P. Lau, *J Mater Chem C*, 2013, 1, 4908-4915.
39. J. Liang, Y. Jiao, M. Jaroniec and S. Z. Qiao, *Angew Chem Int Edit*, 2012, 51, 11496-11500.
40. Z. Yang, Z. Yao, G. F. Li, G. Y. Fang, H. G. Nie, Z. Liu, X. M. Zhou, X. Chen and S. M. Huang, *Acs Nano*, 2012, 6, 205-211.
41. Z. Yang, M. H. Xu, Y. Liu, F. J. He, F. Gao, Y. J. Su, H. Wei and Y. F. Zhang, *Nanoscale*, 2014, 6, 1890-1895.